Tilting multicopter rotors for increased power efficiency and yaw authority

Conrad Holda[1], Behnam Ghalamchi[1,2], and Mark W. Mueller[1]

Abstract— **We demonstrate that a simple mechanical modification increasing the yaw authority of a multicopter leads to a reduction in mechanical power consumption in flight. Increased yaw authority is achieved by tilting the propellers' thrust directions in the direction that increases their yaw torque. The power reduction is achieved in noisy environments, where the vehicle experiences external disturbances. This is due to the lower variance in motor forces required for yaw control, and the convex functional relationship between force and power consumed. We present a theoretical analysis motivating a reduction in power consumed to first order in increasing propeller tilt, in addition to increasing agility. Experiments validate the idea, where the measured electric power is used instead of the mechanical power consumption. Experiments are performed on two quadcopters of very different scales, with masses ranging from** $45\mathrm{g}$ **to** $1.15\mathrm{kg}$**, with both showing a power improvement.**

I. Introduction

Unmanned aerial vehicles (UAVs) have continued to demonstrate their efficacy within a wide range of applications. As the usage of UAVs continues to grow, researchers have increased their efforts in optimizing UAV performance, and a primary limitation for current vehicles is their flight time. A reduction in power consumption is thus a significant factor in improved UAV performance as it directly translates to longer potential flight times.

A primary approach to improving efficiency is through novel designs. For example, tail-sitter vehicles utilize vertical propulsion to perform take-off and landing, but use a wing to fly over long distances [1]–[4]. Other designs decrease power consumption by transitioning to a different style of locomotion to reduce the amount of time the UAV is airborne. These hybrid designs allow the vehicle to alternate between modes that are the most optimal for the task being performed. Some researchers incorporate jumping and gliding [5], flying and crawling [6], and flying, rolling, and floating [7]. All of these combinations have the potential to benefit the efficiency of the UAV; however, including two drastically different modes on a single small vehicle may significantly increase its mechanical complexity and total mass, which in turn makes the vehicles a potentially greater safety risk. Other work is motivated by nature, e.g [8] and [9].

The study conducted in this paper proposes a simple mechanical modification to the standard quadcopter design, which is shown to simultaneously increase the vehicle's agility and reduce its power consumption, while requiring no additional actuators or aerodynamic surfaces. The design incorporates tilting the motors at a fixed angle in the direction that increases the yaw torque from the given actuator. This tilting of the motors requires a greater nominal thrust from each motor for the vehicle to remain at a hover, which would lead to an increase in power consumption in a disturbance-free world. However, in the realistic case of disturbances and noise acting on the vehicle, the motor tilt allows the multicopter to reject disturbances with smaller thrust variations, due to the greater yaw torque authority. Because the thrust usage of a multicopter is related to the power consumption by a convex function, a greater variance in thrust increases the power consumption of the multicopter. We derive a theoretical basis for the reduction in power consumption, and validate this through experiments. The experiments are done on two vehicles of very different scales, with the larger vehicle's mass 25 times greater than the smaller vehicle.

[1]Mech. Eng. Dept., University of California Berkeley, USA.
[2]Mech. Eng. Dept., Lappeenranta University of Technology, Finland.
{conradholda,behnam.ghalamchi,mwm}@berkeley.edu

II. Modelling

We consider a quadcopter with propellers arranged in a rotationally symmetric pattern about the vehicle's center of mass, as shown in Fig. 1, with the body-fixed coordinate system defined by the triad $\mathbf{1}^B$, $\mathbf{2}^B$, and $\mathbf{3}^B$. Each of the vehicle's four propellers is tilted around the vector that connects the centre of the propeller to the centre of mass, such that the propeller's normal vector $\boldsymbol{e}_i$ is at an angle δ with respect to the body-fixed $\mathbf{3}^B$ direction. For each propeller, the tilt is in that direction that would increase the resulting yaw torque. Thus, in the body-fixed coordinate system, the unit vectors $\boldsymbol{e}_i$ perpendicular to the propeller's planes of rotation

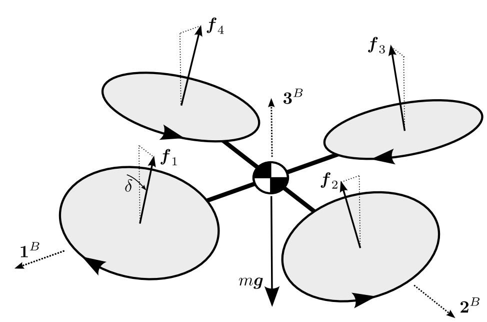

Fig. 1. Diagram of a quadcopter with tilted propellers for increased yaw authority. Each propeller is tilted about the arm connecting to the center of mass by the same angle δ. The propellers are tilted so that their produce a torque about the body-fixed $\mathbf{3}^B$ axis in the same direction as the torque due to the propeller's rotation.

are:

$$\boldsymbol{e}_1 = (0, \sin\delta, \cos\delta)\,, \qquad \boldsymbol{e}_2 = (\sin\delta, 0, \cos\delta) \tag{1}$$

$$\boldsymbol{e}_3 = (0, -\sin\delta, \cos\delta)\,, \quad \boldsymbol{e}_4 = (-\sin\delta, 0, \cos\delta) \tag{2}$$

where we use the short-hand (a, b, c) to denote the components of a vector. Due to their ubiquity, our analysis focuses on quadcopter vehicles, but the analysis may be readily generalized to multicopters with more than four propellers.

A. Dynamics

Each propeller i produces a thrust force $\boldsymbol{f}_i$ and a torque $\boldsymbol{\tau}_i$ as a function of its rotational speed, Ω_i, modeled as below. The torque is referred to the vehicles' center-of-mass, with the vector $\boldsymbol{r}_i$ representing the propeller's displacement (and $\|\boldsymbol{r}_i\| = r$):

$$\boldsymbol{f}_i = \kappa_f \Omega_i^2 \boldsymbol{e}_i \tag{3}$$

$$\boldsymbol{\tau}_i = (-1)^{i+1} \kappa_\tau \boldsymbol{f}_i + S(\boldsymbol{r}_i)\, \boldsymbol{f}_i \tag{4}$$

with κ_f and κ_τ being aerodynamic constants depending on the propellers [10] – this assumes that the propellers are identical up to their handedness. The function $S(\cdot)$ is the skew-symmetric form of its vector argument, so that $S(\boldsymbol{a})\, \boldsymbol{b} = \boldsymbol{a} \times \boldsymbol{b}$ for any vectors $\boldsymbol{a}$ and $\boldsymbol{b}$.

The vehicle's dynamics are compactly described using the Newton-Euler equations. We express its translational acceleration ($\ddot{\boldsymbol{x}}$, in the inertial earth-fixed frame) and its angular acceleration ($\dot{\boldsymbol{\omega}}$, in the body-fixed frame) as below. The vehicle is subject to disturbance forces and torques ($\boldsymbol{f}_d$ and torque $\boldsymbol{\tau}_d$, respectively), expressed in the body-fixed frame. The rotation matrix $\boldsymbol{R}$ relates the body-fixed and earth-fixed frames.

$$m\ddot{\boldsymbol{x}} = m\boldsymbol{g} + \kappa_f \boldsymbol{R} \sum_i \boldsymbol{f}_i + \boldsymbol{f}_d \tag{5}$$

$$\dot{\boldsymbol{R}} = \boldsymbol{R} S(\boldsymbol{\omega}) \tag{6}$$

$$\begin{aligned} \boldsymbol{J}\dot{\boldsymbol{\omega}} =& -S(\boldsymbol{\omega})\, \boldsymbol{J}\boldsymbol{\omega} \\ & + \sum_i \left((-1)^{i+1} \kappa_\tau \boldsymbol{f}_i + S(\boldsymbol{r}_i)\, \boldsymbol{f}_i \right) + \boldsymbol{\tau}_d \end{aligned} \tag{7}$$

wherein m is the mass of the vehicle, $\boldsymbol{J}$ is the mass moment of inertia of the vehicle (expressed in the body-fixed frame), and $\boldsymbol{g}$ is the gravity vector (expressed in the world-fixed frame).

B. Mechanical power consumption

For analysis, we consider only the vehicle's mechanical power consumption, and neglect losses in its electric subsystems (e.g. efficiency of the motors, the electronic speed controllers, etc.). Although these components usually have a large effect on the energy consumption of the vehicle, their design is relatively well understood, and often consists of choosing components from a discrete set (e.g. selecting the model of motor to match a specific propeller choice, and then selecting an electronic speed controller that matches the pair). An example of existing work on optimizing over a discrete set of components is given in [11], and an online calculator for evaluating hobbyist component combinations is given in [12].

The mechanical power p_i of motor i as a function of torque and angular velocity is given by

$$p_i = (\Omega_i \boldsymbol{e}_i)^T \boldsymbol{\tau}_i \tag{8}$$

$$= \frac{\kappa_\tau}{\sqrt{\kappa_f}} \|\boldsymbol{f}_i\|^{\frac{3}{2}} \tag{9}$$

Note that this is the same power relationship as is predicted by actuator disk models of stationary propellers [13].

III. Near-hover analysis

The actuator commands of the vehicle (and thus its mechanical power consumption) near hover comprise of two components: carrying the vehicle weight and providing feedback action to counteract disturbances. In this section, an approximate relationship between the power consumed and the propeller's tilt angle in the presence of noise acting on the system is derived, specifically showing that for any vehicle operating with external disturbances, an increase in propeller tilt angle δ above zero leads to a reduction in power consumed, to first order in δ. Furthermore, the (straight-forward) relationship between the tilt angle δ and the vehicle's maximum angular acceleration about yaw is derived.

A. Near-hover power consumption

For the vehicle to hover, both the acceleration and angular acceleration have to equal zero in expectation, so that a first-order expansion of (5)-(7) gives

$$0 = m\boldsymbol{g} + \kappa_f \boldsymbol{I} \sum_i \mathrm{E}\left[\boldsymbol{f}_i\right] + \mathrm{E}\left[\boldsymbol{f}_d\right] \tag{10}$$

$$0 = \sum_i \left((-1)^{i+1} \kappa_\tau \boldsymbol{I} + S(\boldsymbol{r}_i) \right) \mathrm{E}\left[\boldsymbol{f}_i\right] + \mathrm{E}\left[\boldsymbol{\tau}_d\right] \tag{11}$$

where $\mathrm{E}\left[\cdot\right]$ denotes the expectation operator. From this follows that, if the disturbance force and torque are zero-mean, due to the symmetry of the vehicle

$$\mathrm{E}\left[\|\boldsymbol{f}_i\|\right] = \frac{m\,\|\boldsymbol{g}\|}{4\cos\delta} \tag{12}$$

Due to the nonlinear relationship between power consumption and thrust (9), the expected power consumption will not (in general) scale in the same way with the tilt angle δ. Instead, some intuition for this relationship can be gained by making the following two assumptions: first, that the force disturbances are negligible, and second, that the controller knows the torque disturbances in advance so that at each time instance it acts to exactly cancel the disturbance. In this case, one has

$$\kappa_f \sum_i \boldsymbol{f}_i = -m\boldsymbol{g} \tag{13}$$

$$\sum_i \left((-1)^{i+1} \kappa_\tau \boldsymbol{I} + S(\boldsymbol{r}_i) \right) \boldsymbol{f}_i = -\boldsymbol{\tau}_d \tag{14}$$

and therefore that the propeller forces are an affine function of the disturbance torque, with specifically

$$\|\boldsymbol{f}_i\| = a_0 + \boldsymbol{c}_i^T \boldsymbol{\tau}_d \tag{15}$$

for constant scalar a_0 and vector $\boldsymbol{c}_i$. These are given as below, with $\boldsymbol{c}_2$, $\boldsymbol{c}_3$, and $\boldsymbol{c}_4$ following a similar pattern (and omitted for brevity)

$$a_0 = \frac{m\,\|\boldsymbol{g}\|}{4\cos\delta} \tag{16}$$

$$\boldsymbol{c}_1 = \begin{bmatrix} 0 \\ \frac{1}{2(\kappa_\tau \sin\delta - r\cos\delta)} \\ \frac{1}{4(\kappa_\tau \cos\delta + r\sin\delta)} \end{bmatrix} \tag{17}$$

The first-order Taylor series expansion of the instantaneous power consumed is then given by

$$p_i \sim \|\boldsymbol{f}_i\|^{3/2} \tag{18}$$

$$= a_0^{3/2} + \frac{3}{2} a_0^{1/2} \boldsymbol{c}_i^T \boldsymbol{\tau}_d + \frac{3}{8} a_0^{-1/2} \boldsymbol{c}_i^T \boldsymbol{\tau}_d \boldsymbol{\tau}_d^T \boldsymbol{c}_i + \mathrm{hot} \tag{19}$$

where hot refers to higher order terms in $\boldsymbol{\tau}_d$. Assuming that the disturbance torque is zero-mean, has an isotropic variance $\sigma_\tau^2 I$, and that the higher order terms in the expansion are negligible, this allows to compute the expected per-propeller power

$$\mathrm{E}\left[p_i\right] \approx \frac{\kappa_\tau}{\sqrt{\kappa_f}} \left(a_0^{3/2} + \frac{3}{8} a_0^{-1/2} \sigma_\tau^2 \boldsymbol{c}_i^T \boldsymbol{c}_i \right) \tag{20}$$

This equation permits some insights: firstly, it is clear that the power consumption in the presence of noise will increase to first order in the magnitude of the noise σ_τ^2. Secondly, the power consumption can potentially be decreased by decreasing the term $\boldsymbol{c}_i^T \boldsymbol{c}_i$, which is dependent on the thrust tilt angle δ. Substituting all terms, and expanding to first order, noting that all propellers contribute equally, and finally assuming that the moment arm dominates the aerodynamic reaction torque (i.e. $\kappa_\tau \ll r$) gives

$$\mathrm{E}\left[\sum_i p_i\right] \approx \frac{\kappa_\tau \left(\|\boldsymbol{g}\|\, m\right)^{3/2}}{2\kappa_f} + \frac{3\sigma_\tau^2}{16\sqrt{m\,\|\boldsymbol{g}\|}\,\kappa_\tau \kappa_f} - \frac{3\sigma_\tau^2 r}{8\kappa_f \kappa_\tau^2 \sqrt{\|\boldsymbol{g}\|\, m}}\delta \tag{21}$$

Unfortunately, the above is difficult to apply qualitatively when designing a system, because the disturbance torque's stochastic properties are in general unknown, and will likely vary across different environments (e.g. calm vs. windy environments). However, (21) does show that, to first order in a noisy system, a designer can decrease the mechanical power consumed by a vehicle by increasing the propeller tilt angle from zero. Furthermore, the greater the noise acting on the system, the greater this effect would be.

Of course, for sufficiently large δ, the higher order terms will dominate, and from (16) the thrust required to balance the vehicle weight grows without bound as the tilt angle δ tends to $90°$ (and thus the required power also tends to infinity).

B. Peak yaw acceleration

The vehicle's peak yaw acceleration is achieved if two opposing motors produce the maximum available thrust, while the remaining two motors produce the minimum thrust, here denoted with $f_{\max}$ and $f_{\min}$. The disturbance torque $\boldsymbol{\tau}_d$ is neglected in this analysis, and the mass moment of inertia of the vehicle is assumed to be diagonal, and (due to the vehicle symmetry) that it has only two unique entries: $\boldsymbol{J} = \mathrm{diag}(J_1, J_1, J_3)$. The yaw acceleration is computed using (7), noting that the symmetry of the inertia matrix means that the acceleration ω_3 is independent of the components ω_1, and ω_2 (where $\boldsymbol{\omega} = (\omega_1, \omega_2, \omega_3)$).

$$J_3 \dot{\omega}_3 = \begin{bmatrix} 0 & 0 & 1 \end{bmatrix} \sum_i \left((-1)^{i+1} \kappa_\tau \boldsymbol{f}_i + S(\boldsymbol{r}_i)\, \boldsymbol{f}_i \right) \tag{22}$$

$$= (\kappa_\tau \cos\delta + r\sin\delta) \sum_i \left((-1)^{i+1} \|\boldsymbol{f}_i\| \right) \tag{23}$$

$$\leq 2\left(\kappa_\tau \cos\delta + r\sin\delta\right)\left(f_{\max} - f_{\min}\right) \tag{24}$$

$$\approx 2\left(\kappa_\tau + r\delta\right)\left(f_{\max} - f_{\min}\right) + \mathrm{hot} \tag{25}$$

where again hot refers to higher order terms in δ. This shows that, in addition to the decrease in power consumption, increasing the propeller tilt angle from zero degrees will lead to a higher vehicle agility to first order in δ. In fact, unlike the efficiency, the yaw agility will continue to increase for large tilt angles, up to $\delta = 90°$. The first order agility relationship is, of course, closely related to the power relationship – tilting the rotors gives the vehicle more control authority, meaning that it can reject disturbances with lower forces.

IV. Experimental validation

To show an improvement in efficiency more generally, we tested on two platforms: a small size quadcopter (on the scale of $15\mathrm{cm}$ tip-to-tip, with mass $45\mathrm{g}$) and a large quadcopter (on the scale of $70\mathrm{cm}$ tip-to-tip with mass $1.15\mathrm{kg}$). The small quadcopter was tested at three distinct motor tilt angles: 0, 3, and 6°. The large quadcopter was tested at four angles: 0, 3, 6, and 9°. Each of these configurations was tested in at least 5 flights, and each flight lasted 30 seconds. All experiments were done with similar (fully-charged) batteries, to negate varying electrical inefficiencies with varying battery voltage. An on-board, low-level controller runs at $500\mathrm{Hz}$, while an offboard, higher-level controller runs at $50\mathrm{Hz}$. The vehicle's on-board inertial measurement unit, as well as a motion capture system, were used for state estimation.

A. Small quadcopter

Fig. 2 shows the small quadcopter used for measurement, with a total mass of $44.5\mathrm{g}$. To set the motors at the desired angles, four sets of motor mounts were 3D printed. Each set of motor mounts allowed the motors be fixed at the motor tilt angles for the given experiments. The physical parameters of the small quadcopter are presented in Table I.

Each experiment consisted of a simple flight of three stages: takeoff, hovering, and landing. The reported average power consumption was measured during hover stage, averaging over 20s after allowing for transient behavior to settle.

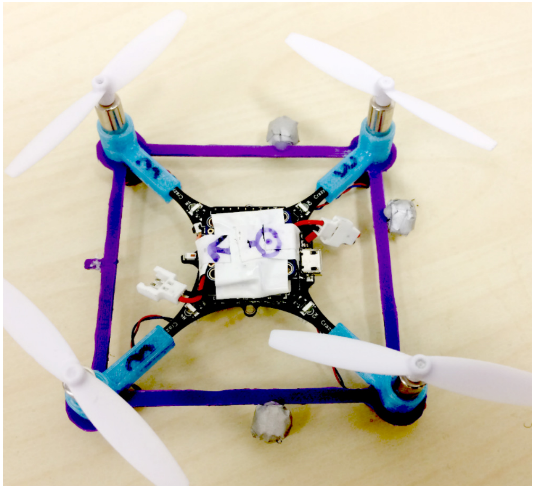

Fig. 2. The small quadcopter used in experiments.

TABLE I

PHYSICAL PARAMETERS OF SMALL QUADCOPTER

Mass	m	44.5gr
Arm length	l	50mm
Aerodynamic constant for angular speed squard to thrust	κ_f	4.14e-8 $\frac{Ns^2}{rad^2}$
Aerodynmaic constant for thrust to torque	κ_τ	0.001
Mass moment of inertia about 1^B axis	J_1	$30e-6kg.m^2$
Mass moment of inertia about 2^B axis	J_2	$30e-6kg.m^2$
Mass moment of inertia about 3^B axis	J_3	$60e-6kg.m^2$

Fig. 3 shows the power measurements during the flight. This test resulted in one data point from the averaged data during the hovering interval of the flight.

Fig. 4 shows the normalized power consumption of small quadcopter. For easier comparison, all reported power consumption values are normalized by the average power consumption when the motors were tilted at $0°$.

From the experimental test results, the small quadcopter saw a 2% decrease in power consumption compared to the traditional, tilt-free configuration. Tilting the motors at $\delta = 6°$ does not show much improvement in power consumption, but still yields a more agile mulitcopter (with an increase in maximum yaw acceleration of 72% compared to the 3 degree motor tilt angle design).

B. Large quadcopter

A second set of experiments was conducted on a larger vehicle, shown in Fig. 5. The vehicle was constructed using a bar with circular cross-section for the motor arms, allowing various motor tilt angles to be set more freely and precisely. The physical parameters of the quadcopter is presented in Table II.

The normalized power consumption for four different tilt angles is presented in Fig. 6. Compared with results for the small quadcopter, the larger vehicle shows less sensitivity to the tilt angle changes, and only a 0.5% improvement in the power consumption efficiency was observed. This may be

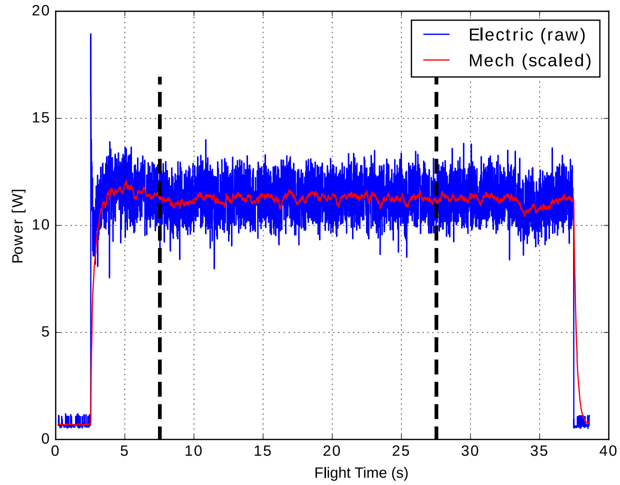

Fig. 3. Recording of the electric power consumption at hover. The value of the power consumption from this flight was obtained using average power consumption for the time between the dotted black lines.

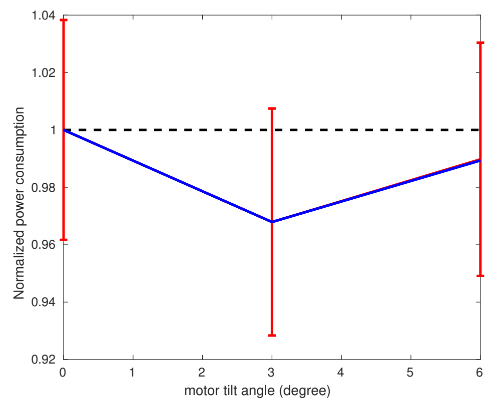

Fig. 4. Normalized power consumption of the small quadcopter. Each dot represents the average power consumption of one flight test and the solid line connects the average power consumption of all tests at each configuration.

reconciled with (21), by examining the term that is affine in tilt angle δ. This term scales inversely proportionally to the aerodynamic constant for thrust to torque squared κ_τ, and inversely proportionally to the square root of the vehicle's mass – as the larger vehicle has both a greater mass and a higher aerodynamic constant κ_τ, a lesser effect is predicted.

Experiments were also conducted where external disturbances were applied using an air blower to disturb the vehicle during flight (thus increasing σ_T in (21)), with the results shown in Fig. 7. As expected, the increase in efficiency was larger for a greater disturbance acting on the quadcopter. Applying additional disturbance to the vehicle, it can be seen that the power consumption decreases around 1.5% at a tilt angle of $3°$. Furthermore, for this tilt angle of $3°$, the large vehicle's maximum yaw acceleration is increased by 72% compared to the tilt-free design. The experiments also showed increased power consumption for larger tilt angles – at these angles the higher order terms of (20) start to dominate.

Fig. 5. The large quadcopter vehicle used in the experiments to test the efficiency of tilted motors. A 15cm ruler is placed in front of the vehicle for scale.

TABLE II

PHYSICAL PARAMETERS OF LARGE QUADCOPTER

Mass	m	1.15kg
Arm length	l	0.225m
Aerodynamic constant for angular speed squard to thrust	κ_f	1.245e-5 $\frac{Ns^2}{rad^2}$
Aerodynmaic constant for thrust to torque	κ_τ	0.0164
Mass moment of inertia about 1^B axis	J_1	$10.6e-6kg.m^2$
Mass moment of inertia about 2^B axis	J_2	$10.6e-6kg.m^2$
Mass moment of inertia about 3^B axis	J_3	$19.4-6kg.m^2$

V. Conclusion

Power efficiency is a primary concern in the design of UAVs, and improvements in efficiency (and thus increases in flight time/range) offer potentially immediate economic advantage. The proposed modification, tilting the thrust axes to increase yaw authority, is shown to decrease power consumption, both through a stochastic analysis, and through experiments. Notably, the power consumption is shown to decrease even though the average thrust force increases. Specifically, the experiments conducted in this study showed power improvements on the order of 2% in hover, with tilt angles on the order of 3°. Future work will consider the effect of the motor tilt on lateral vehicle motions, and on the vehicle's roll and pitch dynamics.

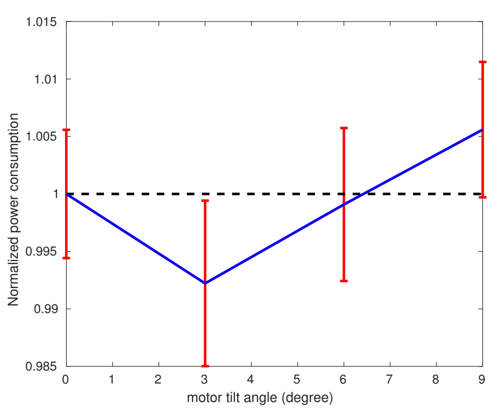

Fig. 6. Normalized power consumption of the custom vehicle. Each dot represents the average power consumption of one flight test and the solid line connects the average power consumption of all tests at each configuration.

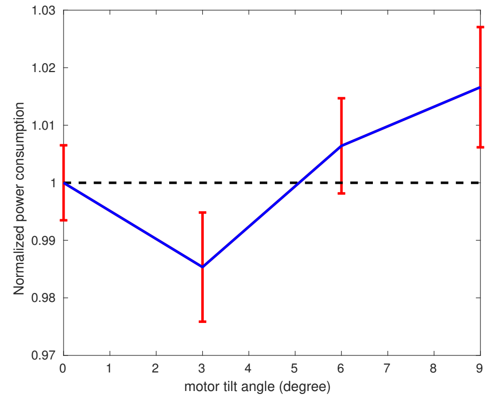

Fig. 7. Normalized power consumption of custom vehicle with additional disturbance from an external air blower. Each dot represents the average power consumption of one flight test and the solid line connects the average power consumption of all tests at each configuration.

VI. Acknowledgement

This work was supported by the UC Berkeley Dept. of Mechanical Engineering, and the Powley Fund. The authors wish to acknowledge Markus Hehn and Flavio Fontana for discussions on the topic of power consumption, and all contributors to the experimental system used (a list is available at `hiperlab.berkeley.edu/members/`), especially Nemo Jin.

References

[1] R. H. Stone and G. Clarke, “Optimization of transition maneuvers for a tail-sitter unmanned air vehicle (UAV),” in *Australian international aerospace congress*, vol. 4, 2001.

[2] D. Kubo and S. Suzuki, “Tail-sitter vertical takeoff and landing unmanned aerial vehicle: Transitional flight analysis,” *Journal of Aircraft*, vol. 45, no. 1, pp. 292–297, 2008.

[3] R. Bapst, R. Ritz, L. Meier, and M. Pollefeys, “Design and implementation of an unmanned tail-sitter,” in *IEEE/RSJ International Conference on Intelligent Robots and Systems (IROS)*, IEEE, 2015, pp. 1885–1890.

[4] R. Ritz and R. D'Andrea, “A global controller for flying wing tailsitter vehicles,” in *IEEE International Conference on Robotics and Automation (ICRA)*, IEEE, 2017, pp. 2731–2738.

[5] M. A. Woodward and M. Sitti, “Multimo-bat: A biologically inspired integrated jumping–gliding robot,” *The International Journal of Robotics Research*, vol. 33, no. 12, pp. 1511–1529, 2014.

[6] L. Daler, J. Lecoeur, P. B. Hhlen, and D. Floreano, “A flying robot with adaptive morphology for multi-modal locomotion,” in *IEEE/RSJ International Conference on Intelligent Robots and Systems (IROS)*, IEEE, 2013, pp. 1361–1366.

[7] K. Kawasaki, M. Zhao, K. Okada, and M. Inaba, “Muwa: Multi-field universal wheel for air-land vehicle with quad variable-pitch propellers,” in *IEEE/RSJ International Conference on Intelligent Robots and Systems (IROS)*, IEEE, 2013, pp. 1880–1885.

[8] J.-H. Han, J.-S. Lee, and D.-K. Kim, “Bio-inspired flapping UAV design: A university perspective,” in *Proc. of SPIE Vol*, vol. 7295, 2009, pp. 72951I-1–72951I-12.

[9] R. J. Wood, “The first takeoff of a biologically inspired at-scale robotic insect,” *IEEE Transactions on Robotics*, vol. 24, no. 2, pp. 341–347, 2008.

[10] P. Pounds, R. Mahony, P. Hynes, and J. Roberts, “Design of a four-rotor aerial robot,” in *Australasian Conference on Robotics and Automation*, vol. 27, 2002, p. 29.

[11] C. Ampatis and E. Papadopoulos, “Parametric design and optimization of multi-rotor aerial vehicles,” in *Applications of Mathematics and Informatics in Science and Engineering*, Springer, 2014, pp. 1–25.

[12] M. Mller. (2017). eCalc – the most reliable electric motor calculator on the web for RC pilots, [Online]. Available: `https://ecalc.ch/` (visited on 08/01/2017).

[13] B. W. McCormick, *Aerodynamics Aeronautics and Flight Mechanics*. John Wiley & Sons, Inc, 1995.